JOURNAL OF Materials CHEMISTRY

Theoretical study of the intercalation of cobaltocene in metal chalcogenides

Anna Ibarz, Eliseo Ruiz and Santiago Alvarez*†

Departament de Química Inorgànica, Universitat de Barcelona, Spain

An electronic band structure study of the intercalation of cobaltocene in SnS_2 and $SnSe_2$ is presented. The preferred position and orientation of the cobaltocene molecules within the host lattices is inferred from a study of the potential energy surfaces, and the orbital interactions that determine the structural preference are analyzed by means of the crystal orbital displacement (COD) functions.

One of the interdisciplinary areas of chemistry which has received a strong momentum in recent years is that of the intercalation compounds of organometallic molecules in layered inorganic solids.[1–3] In such compounds, the guest molecules are bound to the host lattice through weak interactions that make the intercalation process reversible. This means that intercalation and deintercalation reactions proceed under mild conditions. Since the incorporation of guest molecules often result in changes in the physical properties of the host lattice, the preparation of intercalation compounds is foreseen as a low energy-demanding way to tailor the properties of interesting materials. Despite the considerable research devoted to unravel the structure and properties of these compounds, there still remains some controversy over the orientation of the guest molecules and the electronic processes which occur between the guest molecules and the host lattice,[2] neither has a detailed study of the electronic structure of such compounds been reported.

The metal chalcogenides MX_2 are layered compounds with strong M—X bonds within the layers and weak van der Waals interactions between the layers. Some examples of sandwich molecules intercalated in metal chalcogenides include cobaltocene and chromocene in[4,5] TiS_2, $TiSe_2$, TaS_2, $TaSe_2$, ZrS_2, $NbSe_2$ and SnS_2 (in the latter case chromocene is not intercalated but reacts with the chalcogenide[6]), as well as $Mo(\eta^6\text{-}C_6H_6)_2$ and $Cr(\eta^6\text{-}C_6H_6)_2$ in ZrS_2 or TaS_2.[7,8] Ferrocene appears to be more difficult to intercalate, although its intercalation in MoS_2 has been achieved[9] and substituted ferrocene has been intercalated[10] in TaS_2. Even bulkier sandwich complexes such as $Mo(\eta^6\text{-}C_6H_5Me)_2$, $Mo(\eta^6\text{-}C_6H_3Me_3)_2$, $Cr(\eta^5\text{-}C_5H_5)(\eta^7\text{-}C_7H_7)$, $Ti(\eta^8\text{-}C_8H_8)(\eta^5\text{-}C_5H_5)$ or $Co(\eta^5\text{-}C_5H_4R)_2$ ($R = Me, Pr^i, Bu^n$) have been successfully intercalated[7] in ZrS_2. Intercalation compounds of cobaltocene in mixed layer compounds of the type $(MX)_n(TX_2)_2$, such as $(PbSe)_{1.12}(NbSe_2)_2$, $(PbS)_{1.18}(TiS_2)_2$ or $(PbS)_{1.14}(TaS_2)_2$ have also been reported.[11,12] In such compounds the X-ray diffraction data show that the organometallic molecules are placed between two TX_2 layers, while the MX/TX_2 gap remains empty, thus indicating a strong selectivity of the metal dichalcogenide layers for the intercalation of the metallocene.

The intercalation of metallocenes induce interesting changes in the electrical properties of the metal chalcogenide hosts. Thus, electrical resistivity measurements show that the semiconducting ZrS_2 becomes metallic below 30 K when $CoCp_2$, $CrCp_2$ or $Ti(\eta^8\text{-}C_8H_8)(\eta^5\text{-}C_5H_5)$ are intercalated.[11] Intercalation of $CoCp_2$ or $CrCp_2$ in TaS_2 increases the superconducting critical temperature of this sulfide from 0.6 to 3.2 and 2.9 K, respectively.[5] The semiconducting SnS_2 decreases its activation energy upon intercalation of cobaltocene, and the conductivity becomes less anistropic.[6,12–15] $SnSe_2$, a semiconductor with a low activation energy and metallic behavior below 150 K, is metallic at all temperatures when cobaltocene is intercalated, showing a superconducting transition at $T_c = 7.3$ K.

As for the magnetic properties of intercalated metallocenes, all of them follow the Curie–Weiss law. The effective magnetic moment of these compounds can provide some hints on the oxidation state of the metal atom in the metallocene. When the magnetic moment is significantly different from the expected value, a partial charge transfer is assumed and the corresponding degree of oxidation of the metallocene molecules is estimated. As an example, consider the case of $Mo(\eta^7\text{-}C_7H_7)(\eta^5\text{-}C_5H_4Me)$ intercalated in ZrS_2, for which the experimental magnetic moment is 0.58 μ_B, to be compared with an expected value of 0.8 μ_B,[16] compatible with a charge transfer of 53%. For $CoCp_2$ intercalated in SnS_2 and $SnSe_2$, the EPR, XPS, and ^{119}Sn Mössbauer spectra[6,15,17] show that the oxidation of $CoCp_2$ is partial, giving place to mixed valence compounds. The intercalation compound $SnS_2(CoCp_2)_{0.25}$ is paramagnetic with an effective magnetic moment smaller than that expected for all the cobaltocene molecules in the Co^{II} oxidation state, suggesting that only 25% of the molecules remain unoxidized.[12,13] Also upon intercalation of $CoCp_2$, $CrCp_2$, $Ti(\eta^8\text{-}C_8H_8)(\eta^5\text{-}C_5H_5)$, $Mo(\eta^7\text{-}C_7H_7)(\eta^5\text{-}C_5H_4Me)$ or $W(\eta^7\text{-}C_7H_7)(\eta^5\text{-}C_5H_4Me)$ in ZrS_2,[11,16] a partial charge transfer from the organometallic molecule to the host lattice has been detected. Finally, the electron transfer is complete when $CoCp_2$ or $CrCp_2$ is intercalated in TaS_2 (*i.e.*, only $CoCp_2^+$ or $CrCp_2^+$ exist in the intercalation compound).[5] Also a complete oxidation of $CoCp_2^+$ has been deduced from the XPS spectrum[18] upon intercalation in the misfit layer compound $(PbSe)_{1.12}(NbSe_2)_2$.

For all the above reasons, a theoretical study of the electronic structure of intercalation compounds of cobaltocene in metal sulfides and selenides seems interesting. An understanding of the electronic structure of these compounds should allow us to rationalize the orientation of the metallocene molecule within the host lattice and provide some predictions on the most stable positions. Also, a better understanding of the nature of the host–guest interactions should be useful for future experiments to be planned. The crystal and electronic structures of the host compounds have been studied previously at the periodic *ab initio* level.[19] In this paper we report a tight-binding study of the electronic structure of cobaltocene intercalated in SnS_2 and $SnSe_2$. We pay special attention to the position that the cobaltocene molecules occupy within the host lattice and on their relative orientation. Then we will study the most significant orbital interactions in the most stable and

---

† E-mail: salvarez@kripto.qui.ub.es

in the most unstable geometries. By looking at the differences in their electronic structures, we expect to learn about the nature of the host···guest interactions, how they contribute to the stability of the intercalation compounds and what role they play in determining their structures.

Description of the structures

The host structures of SnX_2 ($X=S$, Se) are of the CdI_2 type (Fig. 1), with only one MX_2 formula unit per unit cell. Each metal atom is surrounded by six anions with an approximately octahedral coordination sphere whereas each anion is coordinated to three metal atoms with a trigonal pyramidal geometry. The neighboring layers are stacked in such a way that a metal atom is above another metal atom of the lower layer. In all these intercalation compounds, the stoichiometric host:guest ratio is approximately 4:1.[4,20] Therefore, we will consider four SnX_2 units in the unit cell (*i.e.*, a $2\times2\times1$ supercell relative to the primitive one), represented in Fig. 2(a), where one metallocene molecule per unit cell is also shown. For simplicity we will depict from here on one quarter of the unit cell in which the metallocene is located [Fig. 2(b)] and will schematically represent the host lattice and the metallocene molecule as in Fig. 2(c).

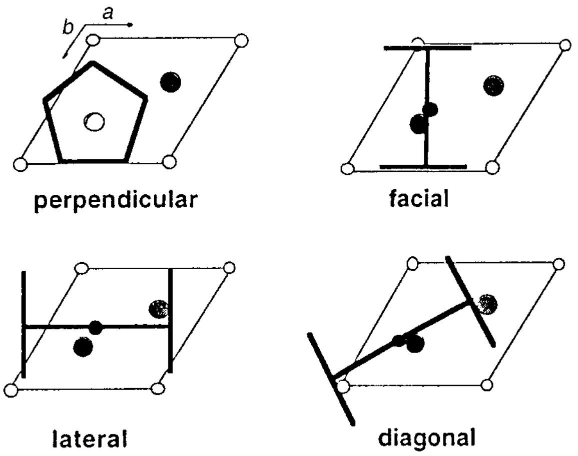

Fig. 3 Schematic illustration of the perpendicular direction of the intercalated metallocene (a) and of three different orientations in the parallel direction: facial (b), lateral (c) and diagonal (d). Definitions as in Fig. 2.

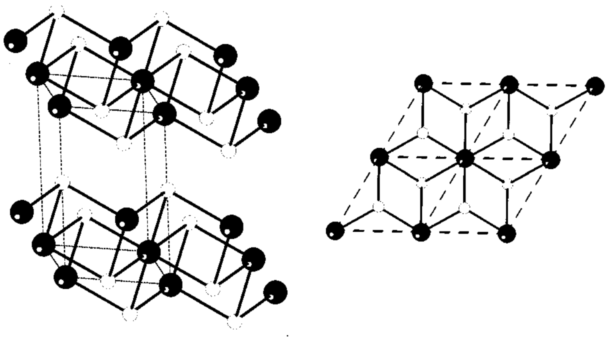

Fig. 1 Perspective view (left) of the structure of SnS_2 (large spheres represent Sn, small ones S atoms) and projection on the *ab* plane (right)

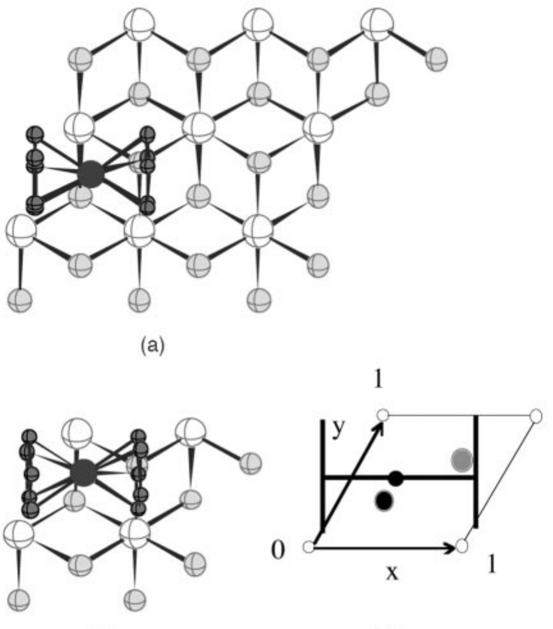

Fig. 2 (a) Unit cell considered for the intercalation compounds $SnX_2(CoCp_2)_{0.25}$ ($X=S$, Se), where the black spheres represent the cobaltocene molecule. The portion of the unit cell in which the $CoCp_2$ is located (b) is subsequently depicted in a schematic way (c).

We choose to define the arrangement of the intercalated metallocene molecule between the host layers by three parameters: position, direction and orientation. The position of the centroid of the metallocene within the studied portion of the unit cell can be defined by its two orthogonal coordinates *x* and *y*, where *x* is directed along the crystallographic *a* axis. Two most likely directions for the molecular C_5 symmetry axis can be foreseen: perpendicular to the layer direction [Fig. 3(a)], or parallel to it [Fig. 3(b)–(d)]. For the perpendicular direction of the metallocene, different orientations can be generated by rotation around the *c* axis, but we will consider only the three most symmetric ones: facial [Fig. 3(b)], lateral [Fig. 3(c)] and diagonal [Fig. 3(d)]. Early attempts to determine the direction of the intercalated molecules were based on the X-ray and neutron diffraction patterns of polycrystalline samples, by comparing the interlayer separation in the intercalation compound with that of the precursor metal chalcogenide, and assuming that the dimension of the $CoCp_2$ molecule is larger along the pentagonal axis (*ca.* 6.8 Å) than in the perpendicular direction (*ca.* 5.6 Å).[4] Later studies showed that the dimensions of the cobaltocene molecule in the two directions are quite similar (6.96 and 6.74 Å, respectively),[8,21] making the analysis of the powder diffraction data inconclusive. More recently, variable temperature solid state ^2H NMR studies[22–26] have allowed one to distinguish between the parallel and perpendicular directions of the intercalated metallocenes. In particular, cobaltocene has been found to adopt the parallel arrangement when intercalated in metal sulfides or selenides. Conversely, ferrocene intercalates in MoS_2 with a perpendicular arrangement, and so do the Mo compounds in ZrS_2.[9,22] However, the position inside the unit cell and the relative orientation of organometallic molecules in successive layers remain unknown.

One must be aware of the existence of experimental evidence that different directions and orientations of the intercalated metallocene have small energy differences. Both the ^1H and ^2H NMR variable temperature spectra have been used to obtain information on the dynamic behavior of the intercalated molecules.[27] Thus, the activation energy for the rotation of the cobaltocene molecule from the parallel to the perpendicular orientation in $2H\text{-}TaS_2(CoCp_2)_{0.25}$ has been estimated to be 8.2 kcal mol^{-1} from the ^1H spectra and 6.1 kcal mol^{-1} from the ^2H spectra,[24,27] whereas the barrier for rotation around the pentagonal axis has been estimated to be only 0.1 kcal mol^{-1}.[27]

Intercalation of cobaltocene in SnS_2 and $SnSe_2$

In this section we present the results of a theoretical tight-binding band structure study of the intercalation compounds $SnX_2(CoCp_2)_{0.25}$ ($X = S$, Se). In our previous work[19] we have shown through *ab initio* band calculations on the ionic intercalation compounds $SnX_2Li_{0.25}$ that the energy required to separate the layers of the host lattice is quite small (1–2 kcal mol^{-1}), whereas the energy gain upon reducing the layer (-147 and -158 kcal mol^{-1} per M_4X_8 unit cell for $X = S$ and Se, respectively) is larger than that required to oxidize the cobaltocene molecule ($+130$ kcal mol^{-1}). It is clear that the electron transfer between the metal-centered e_{1g} orbital of the cobaltocene guest molecule to the 5s (Sn) orbital of the SnX_2 host lattice provides a driving force for the intercalation. Semiempirical band calculations of the extended Hückel (EHTB) type[28–30] cannot adequately describe such charge transfer processes, given the neglect of the two-electron terms and their exaggeration of the destabilization of antibonding levels. However, *ab initio* calculation of the host···guest interaction in $SnX_2(CoCp_2)_{0.25}$ is not attainable at the present time with HF-based methods and we have adopted the semiempirical approach for a qualitative study the host···guest interactions in these intercalation compounds. In so doing, one must be careful not to only draw conclusions that may depend on the occupation of the orbitals involved in the charge transfer process.

First we will check the results of the EHTB calculations on the host lattice of SnS_2 with our previous *ab initio* results on the same system. We will then try to obtain some hints as to the more likely position and orientation of cobaltocene intercalated in SnS_2 and $SnSe_2$. For the most likely geometries, we will discuss in detail the electronic structure of the intercalation compound and analyze the host–guest interactions by means of the COD (crystal orbital displacement) curves[31] used successfully in previous works for the study of weak interactions in the solid state. Finally, an orbital analysis of the host···guest interaction should allow us to provide a simple description of those interactions. The study of the guest···guest interactions is of interest also to understand their influence on the energetics and geometry of the intercalation compounds. It is in particular interesting to investigate whether the guest molecules are expected to have the same orientation or be disordered. However, such study can be carried out at a more accurate level of theory by studying bimolecular models, and will be undertaken separately.[32]

The electronic structure of the host lattices has been studied at the Hartree–Fock *ab initio* level in a previous paper[19] and discussed in detail there. We only present here the density of states of SnS_2 calculated at the HF level, to show that the results of the EHTB calculations are qualitatively comparable with the *ab initio* ones, and that these calculations can be reasonbly used to study the intercalation compounds (Fig. 4). In the two cases the lowest band has mostly sulfur 3s character, the valence band is essentially sulfur 3p with small contributions from the metal atoms, and the conduction band presents contributions from both the Sn and S atoms. The atomic orbital contributions (not shown in the figure) to the different bands are similar in the two types of calculations. The two most important differences between the two DOS plots are a slightly larger bandwidth, and a larger forbidden energy gap in the HF case. Since it is known that the energy gap is overestimated by the HF calculations, and there are not significant differences between the qualitative description of the electronic structure provided by the two methods, we conclude that it is sensible to employ the EHTB method for the study of the intercalation compounds, which cannot at present time be carried out at the *ab initio* level, due to computational limitations.

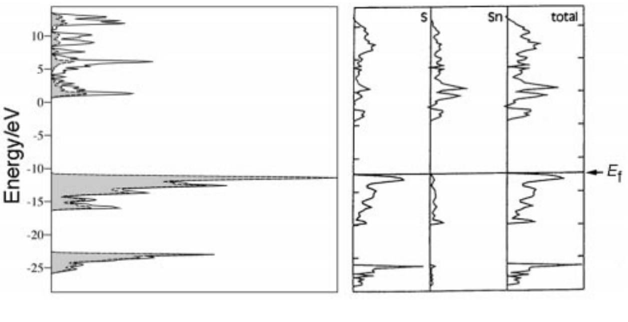

Fig. 4 Total density of states for SnS_2 as obtained from EHTB (left) and HF (right) calculations. The contribution of the S atoms to the DOS in the EHTB curve is represented by the shaded area, and the contributions of the Sn and S to the DOS in the HF curve are plotted separately.

The calculated one-electron energy surfaces (see Appendix for computational details) for $SnX_2(CoCp_2)_{0.25}$ are presented in Fig. 5 ($X = S$) and 6 ($X = Se$) as a function of the x and y coordinates ($0 < x,y < 1$, within the section of the unit cell shown in Fig. 3) of the cobaltocene molecule at four different orientations. The relative energies of the maxima and minima of such surfaces are presented in Table 1. The same qualitative behavior is found for the two host lattices, in the sense that the maxima and minima in the potential energy surface correspond to the same positions of the intercalated cobaltocene molecule. The energy surface is shallower for the selenide than for the sulfide, although it must be kept in mind that the separation between layers is larger in $SnSe_2$ than in SnS_2. The minimum energy positions correspond to the lateral orientation with the Co atom situated in-between two neighboring Sn atoms of the host lattice. However, the energies required to rotate the cobaltocene molecule around the stacking direction in that position are only a few kcal mol^{-1}. In contrast, even the most stable position for the perpendicular orientation is too high in energy (133 and 73 kcal mol^{-1} for SnS_2 and $SnSe_2$, respectively) to be thermally accessible. These results are consistent with the experimental data obtained from ^2H NMR spectra,[14,15,25,26,33] that indicate that cobaltocene intercalated in SnS_2 and $SnSe_2$ adopts a parallel orientation and that a rotation of the sandwich molecules is likely at room temperature. The small energy differences between the several possible parallel orientations is also compatible with the existence of a disordered array of cobaltocene molecules that would render the resolution of the structure by diffraction methods difficult. Even if the numerical results obtained with the EHTB calculations should be taken cautiously, given the approximations involved, previous studies on intercalation compounds, such as the Hofmann clathrates or the alkali halide-intercalated halogens, show that a wealth of structural and spectral data can be accounted for by these calculations.[31,34,35] In particular, the orientation of the guest molecules relative to the host lattice is very well reproduced, and explained through weak orbital interactions between host and guest. Even if the potential energy surfaces have been calculated with a half-occupied $e_{1g}(CoCp_2)$ band, we will show in the next section that the host···guest interaction is not affected by the charge transfer from that band to 5s(Sn) of the host lattice, hence all the conclusions drawn from such energy surfaces can be applied to the ionic intercalation compounds $(CoCp_2{}^+)_{0.25}(SnX_2)^{-0.25}$ as well.

In order to check whether the assumption used in the previous calculations, that all the intercalated cobaltocene molecules adopt the same orientation, is a sensible one, we performed calculations for a system with a larger unit cell containing four $CoCp_2$ molecules in a lateral orientation and 16 formula units of SnS_2. The total energy was calculated for three different orientations of one of the cobaltocenes relative to the other three and found to be larger when one cobaltocene is rotated than when all the cobaltocenes are parallel (31 and

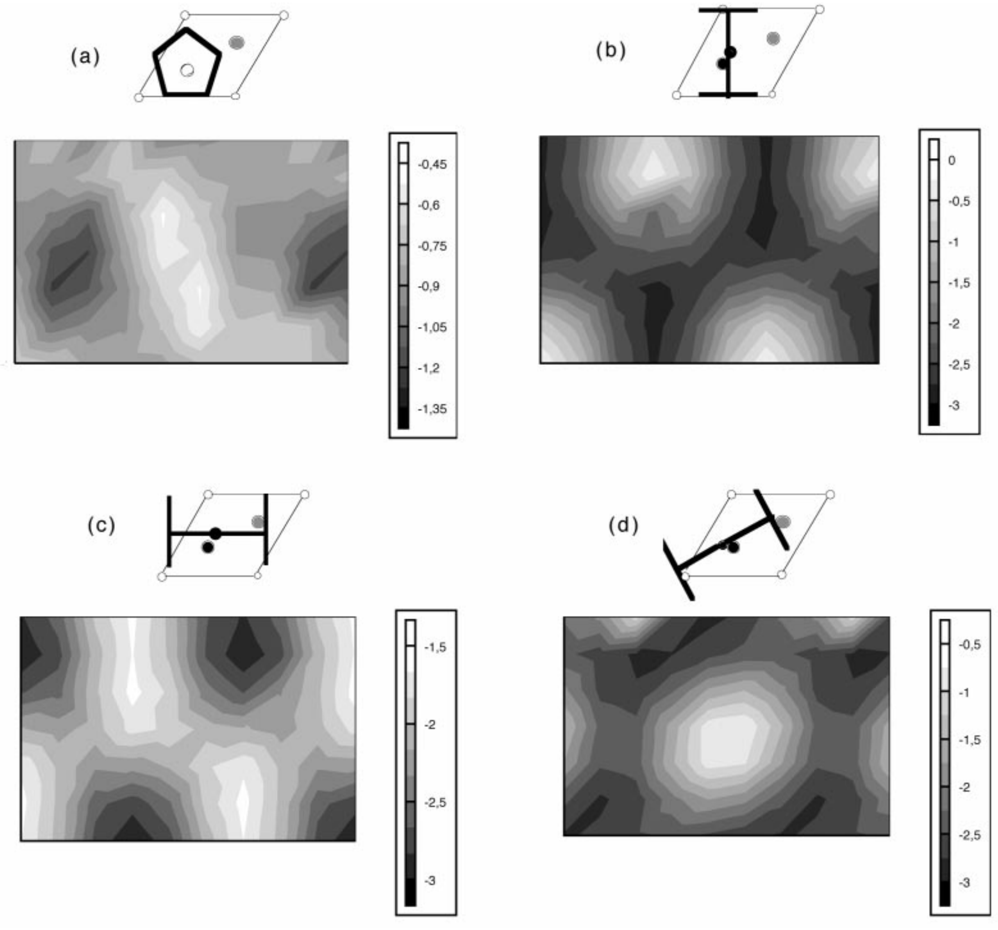

Fig. 5 One-electron potential energy surface (eV) for the perpendicular (a), facial (b), lateral (c) and diagonal (d) orientations of the cobaltocene molecule in $SnS_2(CoCp_2)_{0.25}$. Coordinates and energies for the minima and maxima are given in Table 1.

56 kcal mol^{-1}, for rotation angles of 60 and 90°, respectively). The same trend was found for the sublattice of cobaltocene molecules, but with smaller energy differences (up to 7 kcal mol^{-1}), suggesting that the orientation of the guest molecules is mostly determined by host···guest interactions.

Electronic structure and host···guest interactions in $SnS_2(CoCp_2)_{0.25}$

We will now focus on the structure predicted to be more stable, namely the lateral orientation with the cobalt atom in the (0, 1/2) position, in order to analyze how the electronic structure of the host lattice is affected by the intercalation and to find out why this geometry is more stable. We limit such analysis to the tin sulfide intercalate, which is the one expected to show stronger van der Waals interactions[19] and a more pronounced geometry preference. The total density of states (DOS) of $SnS_2(CoCp_2)_{0.25}$ is presented in Fig. 7, together with the contribution of the cobaltocene molecules. For a single cobaltocene molecule, one should expect the d-block orbitals to be split into three low-energy orbitals (e_{2g} and a_{1g}) and two metal–ligand antibonding e_{1g} orbitals.[36] For the neutral cobaltocene, with a d^7 electron configuration, one unpaired electron should be placed in the e_{1g} orbitals. Accordingly, in the DOS diagram, the peak slightly above -10 eV, crossed by the Fermi level, is built up from the e_{1g} orbitals of cobaltocene. Comparison of the DOS of the intercalation compound with that of the host lattice (Fig. 4) and with the molecular orbitals of $CoCp_2$[36] allows us to identify each DOS peak with the levels of the two sublattices. Except for the presence of the peaks associated with the cobaltocene sublattice, the DOS peaks for the intercalation compound look the same as those for the SnS_2 lattice, suggesting that the electronic levels of the intercalation compound are just a superposition of those of its constituents without modification.

Notice that the one-electron description of the electronic structure is not able to account for the electron transfer from $CoCp_2$ to the host, probably due to the neglect of two-electron terms in the EHTB calculations. However, since we know from the experimental data that such electron transfer occurs, it is clear that it should go from the e_{1g} orbital of $CoCp_2$ to the 5s(Sn) band of SnS_2, in agreement with the metallic character found for $SnS_2(CoCp_2)_{0.25}$. Therefore, in the subsequent discussion we must be careful not to draw any conclusion that may depend on the relative occupations of those two bands.

Despite the apparent constancy of the electronic structure upon intercalation, weak interactions between a few orbitals of the host and guest may be masked among the wealth of non-interacting orbitals. Hence, an appropriate analysis of the electronic structure of an intercalation compound consists in plotting the crystal orbital displacement (COD) curves that get rid of the non-interacting orbitals and show only those levels that are affected by the host–guest interaction.[31,37] In a COD curve for a given orbital we represent the difference between its contribution to the DOS of the intercalation compound and to the DOS of the isolated guest sublattice. In such way, the non-interacting levels are removed, and those levels that are displaced upon intercalation give a positive peak in the energy region at which they appear after intercalation and a negative peak in the region at which they appeared previous to intercalation. If the COD curve for a particular orbital is integrated up to the Fermi level, the resulting value, ICOD(E_F) indicates the net change in electron population for that orbital upon intercalation.

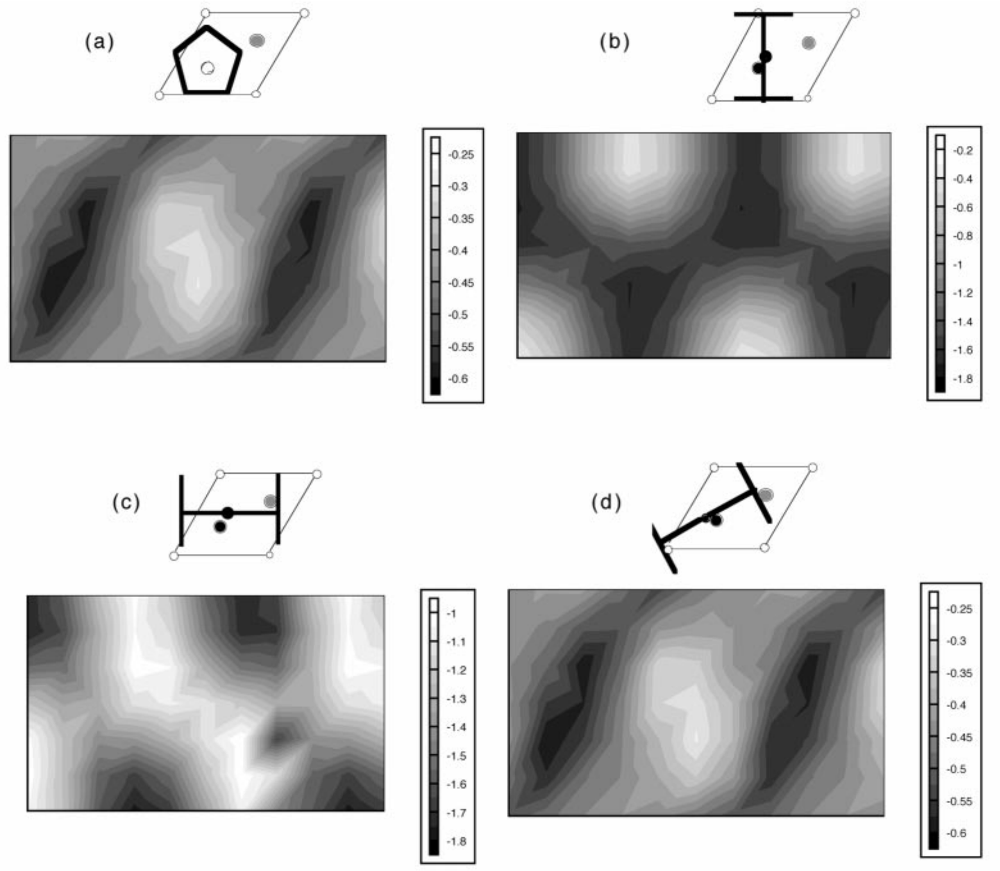

Fig. 6 One-electron potential energy surface (eV) for the perpendicular (a), facial (b), lateral (c) and diagonal (d) orientations of the cobaltocene molecule in $SnSe_2(CoCp_2)_{0.25}$. Coordinates and energies for the minima and maxima are given in Table 1.

Table 1 Positions and relative energies (kcal mol^{-1}) of the minima and maxima in the potential energy surfaces for the four orientations of the metallocene in $SnX_2(CoCp)_{0.25}$ (X = S, Se)

orientation	position (*x*,*y*)	*E* (SnS_2)	*E* ($SnSe_2$)
minima			
perpendicular	(0.67, 0.17)	133.0	73.1
facial	(0.33, 0.0)	2.1	1.1
lateral	(0.0, 0.50)	0.0	0.0
diagonal	(0.0, 0.17)	4.3	3.3
maxima			
perpendicular	(0.33, 0.67)	149.1	79.3
facial	(0.0, 0.0)	62.9	32.5
lateral	(0.0, 0.0)	30.4	16.7
diagonal	(0.17, 0.83)	51.2	26.2
other			
perpendicular	(0.0, 0.50)	141.1	77.1
facial	(0.0, 0.50)	3.9	2.5
diagonal	(0.0, 0.50)	1.2	5.4

Comparison of the ICOD(E_F) values for the molecular orbitals of cobaltocene in its most stable (lateral) with those in the most unstable (perpendicular) orientation shows that the cobalt 3d orbitals are little affected by the host···guest interaction. In contrast, the ICOD(E_F) values for the bonding and antibonding orbitals of the Cp rings (Table 2) tell us that for the stable lateral orientation the most important interaction affects the σ*(C—H) orbitals of Cp, which gain electron density upon intercalation (positive value). Which orbitals of the host lattice interact with the σ*(C—H) orbitals of the Cp rings? This question can be answered by looking at the COD curve for these MOs (Fig. 8), in which the two peaks coincide with the sulfur 3s (below) and 3p (above) bands of the SnS_2 lattice (Fig. 4). In brief, the interaction contributing to the stability of the intercalation compound and favoring the lateral

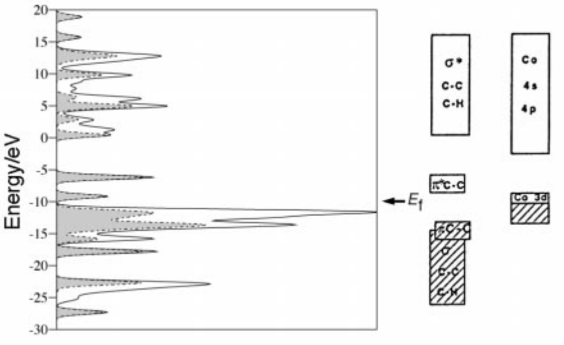

Fig. 7 Total density of states and contribution of the cobaltocene orbitals (shaded areas) for $SnS_2(CoCp_2)_{0.25}$ in the lateral orientation of $CoCp_2$ at the (0, 1/2) position. The energies of the different molecular orbitals[36] of a $CoCp_2$ molecule and of the bands of SnS_2 are shown as a block diagram (shaded blocks indicate occupied levels).

Table 2 Values of the integrated COD curves up to the Fermi level, ICOD(E_F) ($\times 10^4$) for the cobaltocene molecular orbitals in the stable lateral and unstable perpendicular orientations at the position (0, 1/2) of the cobalt atom. The orbitals are grouped according to their bonding characteristics and the number of orbitals in each group is indicated by its multiplicity

MO	multiplicity	lateral	perpendicular
σ(C—H)	14	−1	−24
π(C—C)	6	−1	−432
π*(C—C)	4	14	700
σ*(C—H)	16	618	182

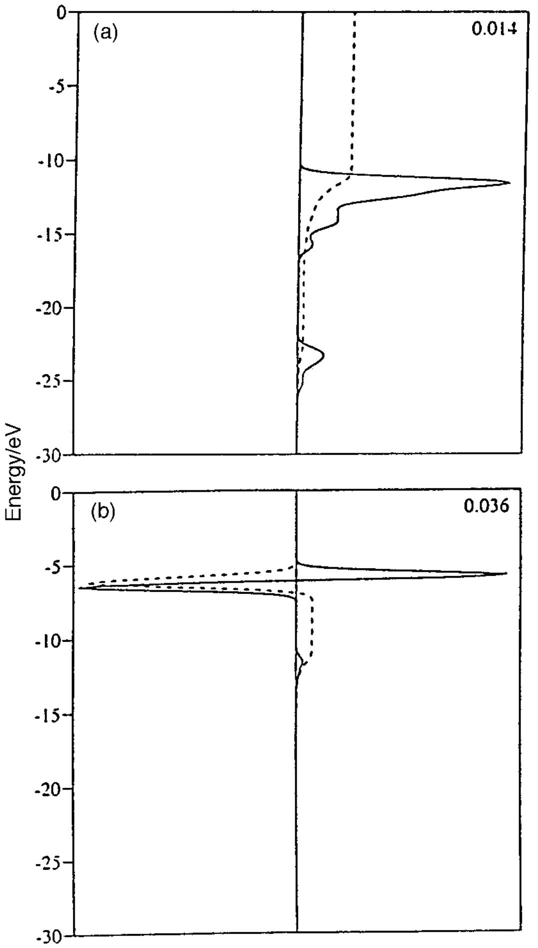

Fig. 8 COD (solid line) and ICOD (dashed line) curves for the (a) σ^*(C—H) and (b) π(Cp) molecular orbitals of $CoCp_2$ upon intercalation in the lateral orientation. The number in the upper right corner indicates the maximum of the scale for the COD curve, and the Fermi level is at −9.2 eV.

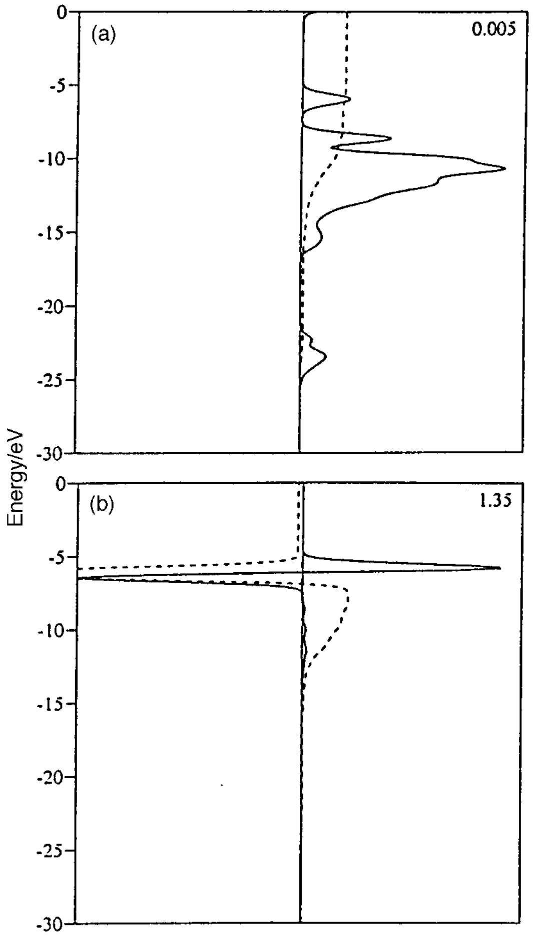

Fig. 9 COD (solid lines) and ICOD (dashed lines) curves for the (a) σ^*(C—H) and (b) π^*(C—C) orbitals of cobaltocene intercalated in SnS_2 with a perpendicular orientation. Only the energy window below the Fermi level is shown. The number in the upper right corner indicates the maximum of the COD scale.

orientation can be described as an electron density donation from the sulfur lone pairs pointing to the van der Waals gap toward the σ^*(C—H) orbitals of the Cp rings or, in other words, a weak hydrogen bond of the C—H···S[38] type represented at the orbital level in **1**. Notice that neither the e_{1g}($CoCp_2$) nor the 5s(Sn) levels, involved in the charge transfer, have an important contribution to the host···guest interactions. Hence the conclusions of our study are not affected by the poor description of the charge transfer process by our one-electron band calculations.

A similar analysis can be carried out for the cobaltocene molecule perpendicularly oriented in the SnS_2 lattice and in the same position as above, which corresponds to one of the least stable situations. The values of the ICOD functions at the Fermi level (Table 2) show again that the two most important interactions are those of the host sulfur atoms with the σ^*(C—H) and π^*(C—C) orbitals of the guest. The difference is that in this case the interaction of the σ^*(C—H) orbital with the host lattice is much weaker, as should be expected for C—H···S interactions in this orientation. A look at the COD curves (Fig. 9) shows that the σ^*(C—H) system interacts less with the p(S) bands and that new levels appear at higher energy, above the Fermi level. The strongest interactions in this case occur *via* the π^*(C—C) and π(C—C) orbitals [Table 2 and Fig. 9(b)]. Although the ICOD(E_F) values indicate that there are stronger $S^{2-} \rightarrow \pi^*$(Cp) and π(Cp)→host donations with the cobaltocenes arranged in a perpendicular than in a lateral orientation, the intercalate is computationally more

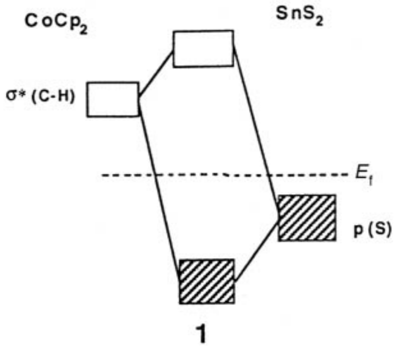

1

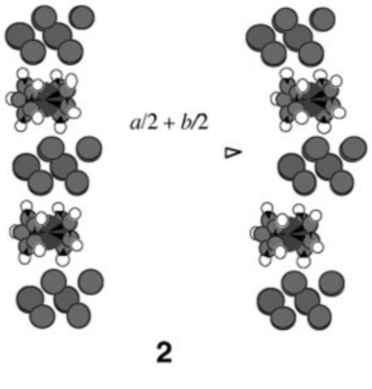

2

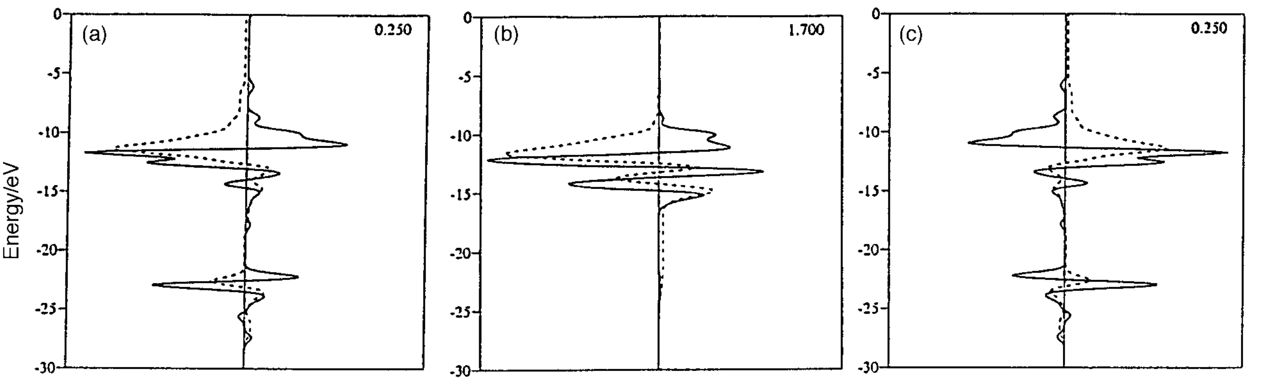

Fig. 10 Crystal orbital displacement (COD, solid line) and ICOD (dashed line) curves for the (a) sulfur atomic orbitals of the intercalation compound $SnS_2(CoCp_2)_{0.25}$ in the perpendicular orientation, relative to the pristine host lattice, (b) analogous COD for the π(Cp) orbitals of cobaltocene, and (c) sulfur atomic orbitals in the lateral intercalation compound relative to the perpendicular one. The number in the upper right corner indicates the scale for the COD function.

stable in the second case. The reason for this apparent contradiction is that in the perpendicular orientation the stronger stabilizing interactions are combined with stronger repulsion between occupied orbitals of the host and guest sublattices. This can be illustrated by another set of COD diagrams, where, we can see [Fig. 10(a)] that the sulfur 3p band at around −10 eV is broadened upon intercalation, as indicated by an increase in the number of levels at low and high energies (positive sign of the COD curve at −14 and −10 eV) and a decrease in the number of levels at intermediate energies[31] (note that a broadened band is the solid state version of a two orbital–four electron repulsion in a molecular system). A similar broadening [Fig. 10(b)] and the subsequent destabilization can be found for the occupied bands of the π(Cp) system. Finally, a COD curve comparing the sulfur density of states in the lateral and perpendicular orientations [Fig. 10(c)] clearly shows that the sulfur 3p bands appear at higher energy in the latter case (negative peak around −10 eV).

We have so far assumed a perfect stacking of the layers in the intercalation compounds. However, it has been experimentally found that a doubling of the unit cell along the *c* direction results in some cases upon intercalation. In the case of $SnS_2(CoCp_2)_{0.25}$,[33] the successive host layers are displaced by $(a+b)/2$, and in $TaS(CoCp_2)_{0.25}$[22] by $(a+b)/3$ (**2**). We have carried out EHTB calculations with the doubled unit cell and with the successive layers shifted by an $m(a+b)$ vector for $SnS_2(CoCp_2)_{0.25}$, where *m* was varied between 0 and 2/3 (*a* and *b* here refer to the primitive unit cell of the host lattice). The calculated one-electron energy is plotted as a function of *m* in Fig. 11. There it is seen that two minima appear, one with the regular stacking assumed in our previous calculations, and another one with similar energy for $m=1/2$, consistent with the experimental data. This result suggests that different layer stacking sequences may have similar energies and the resulting structures may be incommensurate or disordered along the *c* direction.

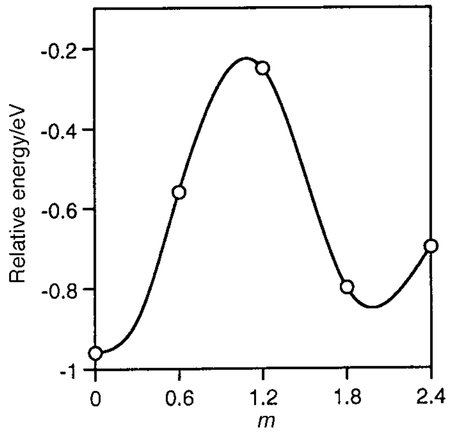

Fig. 11 Calculated relative energy as a function of the shift vector $m(a+b)$ between successive layers, in $SnS_2(CoCp_2)_{0.25}$ with a doubled unit cell along the *c* axis

Concluding remarks

The EHTB calculated energy surfaces for $SnX_2(CoCp_2)_{0.25}$ (X = S, Se) are similar, give a minimum for a structure in which the Co atom is midway between two Sn atoms along the *b* direction and the molecular C_5 axis of $CoCp_2$ is parallel to the crystallographic *a* direction. The perpendicular orientation is predicted to be very high in energy, whereas other parallel orientations are only a few kcal mol^{-1} higher than the minima. This result suggests the possibility of rotational disorder of the intercalated cobaltocene molecules.

The analysis of the COD and ICOD functions indicates that the cobalt 3d orbitals are little affected by the host···guest interaction. In the preferred lateral orientation, the most important interaction can be described as a donation from the sulfide lone pairs pointing to the van der Waals gap toward the σ*(C—H) orbitals of the cyclopentadienide ligands, or a C—H···S weak hydrogen bonding.

In the perpendicular orientation, there are stronger $S^{2-}\rightarrow\pi^*(Cp)$ and $\pi(Cp)\rightarrow$host donor/acceptor interactions, but these are counterbalanced by strong repulsions between the lone pairs of the sulfides and the occupied orbitals of the cyclopentadienide rings.

Appendix: Computational details

The tight-binding extended Hückel calculations[28–30] were performed with the programs YAeHMOP[39] and EHMACC.[40] In all cases, the modified Wolfsberg–Helmholz formula[41] for the calculation of the off-diagonal terms of the ***H*** matrix was used. The atomic orbital ionization potentials were taken from the tables of Vela and Gázquez,[42] and the Slater exponents from the tables of Alvarez.[43] For the calculation of properties (DOS, COD and energies) a grid of 40 k points from the irreducible set of the Brillouin zone was used, according to the criterion of Ramírez and Böhm.[44,45] The unit cell parameters employed correspond to the experimental values of *a* and *b* for the metal chalcogenide, and those of *c* were taken from the powder diffraction data of the intercalation compounds.[5,15,33,46] For the geometry of the cobaltocene molecule, the following structural parameters were adopted: Co—C = 2.010, C—C = 1.411, C—H = 1.083 Å.

This work has been funded by DGES through the research project PB95–0848-C02–01. The use of the computing resources at the Centre de Supercomputació de Catalunya (CESCA) was supported in part by the Universitat de Barcelona.

References

1 D. O'Hare, in *Inorganic Materials*, ed. D. W. Bruce and D. O'Hare, John Wiley & Sons Ltd, New York, 1996.
2 D. O'Hare and J. S. O. Evans, *Comments Inorg. Chem.*, 1993, **14**, 155.
3 D. O'Hare, *New. J. Chem.*, 1994, **18**, 989.
4 M. B. Dines, *Science*, 1975, **188**, 1210.
5 F. R. Gamble and A. H. Thompson, *Solid State Commun.*, 1978, **27**, 379.
6 D. O'Hare, W Jaegermann, D. L. Williamson, F. S. Ohuchi and B. A. Parkinson, *Inorg. Chem.*, 1988, **27**, 1537.
7 W. B Davies, M. L. H. Green and A. J. Jacobson, *J. Chem. Soc., Chem. Commun.*, 1976, 781.
8 R. N. Clement, W. B. Davies, K. A. Ford, M. L. H. Green and A. J. Jacobsen, *Inorg. Chem.*, 1978, **17**, 2754.
9 H. Tagaya, T. Hashimoto, M. Karasu, T. Izumi and K. Chiba, *Chem. Lett.*, 1991, 2113.
10 K. Chatakondu, C. Formstone, M. L. H. Green, D. O'Hare, J. M. Twyman and P. J. Wiseman, *J. Mater. Chem.*, 1991, **1**, 205.
11 H. Wong, R. Millet, J. S. O. Evans, S. Barlow and D. O'Hare, *Chem. Mater.*, 1995, **7**, 210.
12 C. A. Formstone, E. T. FitzGerald, D. O'Hare, P. A. Cox, M. Kurmoo, J. W. Hodby, D Lillicrap and M. Goss-Custard, *J. Chem. Soc., Chem. Commun.*, 1990, 501.
13 C. A. Formstone, M. Kurmoo, E. M. FitzGerald, P. A. Cox and D. O'Hare, *J. Mater. Chem.*, 1991, **1**, 51.
14 D. O'Hare, C. A. Formstone, E. T. FitzGerald, P. A. Cox and M. Kurmoo, *Synth. Met.*, 1991, **41–43**, 2575.
15 D O'Hare, *Chem. Soc. Rev.*, 1992, 121.
16 M. L. H. Green, K. P. Ng and H. V. Wong, *J. Chem. Soc., Dalton Trans.*, 1993, 3213.
17 C. A. Formstone, E. T. FitzGerald, P. A. Cox and D. O'Hare, *Inorg. Chem.*, 1990, **29**, 3860.
18 L. Hernán, J. Morales, L. Sánchez, J. L. Tirado and A. R. González Elipe, *J. Chem. Soc., Chem. Commun.*, 1994, 1081.
19 A. Ibarz, E. Ruiz and S. Alvarez, *Chem. Mater.*, submitted.
20 B. F. Hoskins, R. Robson and N. V. Y. Scarlett, *J. Chem. Soc., Chem. Commun.*, 1994, 2025.
21 H. Schäfer-Stahl and R. Abele, *Angew. Chem., Int. Ed. Engl.*, 1980, **19**, 477.
22 J. S. O. Evans and D. O'Hare, *Chem. Mater.*, 1995, **7**, 1668.
23 C. Grey, J. S. O. Evans, D. O'Hare and S. J. Heyes, *J. Chem. Soc., Chem. Commun.*, 1991, 1380.
24 S. J. Heyes, N. J. Clayden, C. M. Dobson, M. L. H. Green and P. J. Wiseman, *J. Chem. Soc., Chem. Commun.*, 1987, 1560.
25 S. J. Mason, S. J. Heyes, H. V. Wong and D. O'Hare, *Inorg. Chem.*, 1995, **34**, 4287.
26 H. Wong, J. S. O. Evans, S. Barlow, S. J. Mason and D. O'Hare, *Inorg. Chem.*, 1994, **33**, 5515.
27 B. G. Silbernagel, *Chem. Phys. Lett.*, 1975, **34**, 298.
28 R. Hoffmann, *J. Chem. Phys.*, 1963, **39**, 1397.
29 M.-H. Whangbo and R. Hoffmann, *J. Am. Chem. Soc.*, 1978, **100**, 6093.
30 M.-H. Whangbo, R. Hoffmann and R. B. Woodward, *Proc. R. Soc. London, Ser. A.*, 1979, **366**, 23.
31 E. Ruiz, S. Alvarez, R. Hoffmann and J. Bernstein, *J. Am. Chem. Soc.*, 1994, **116**, 8207.
32 A. Ibarz, E. Ruiz and S. Alvarez, unpublished work.
33 D. O'Hare, J. S. O. Evans, P. J. Wiseman and K. Prout, *Angew. Chem., Int. Ed. Engl.*, 1991, **30**, 1156.
34 E. Ruiz and S. Alvarez, *Inorg. Chem.*, 1995, **34**, 5845.
35 E. Ruiz and S. Alvarez, *J. Am. Chem. Soc.*, 1995, **117**, 2877.
36 T. A. Albright, J. K. Burdett and M.-H. Whangbo, *Orbital Interactions in Chemistry*, John Wiley & Sons, New York, 1985.
37 S. Alvarez, *Rev. Acad. Cienc. Exactas*, 1994, **88**, 353.
38 C. Rovira and J. J. Novoa, *Chem. Phys. Lett.*, 1997, **279**, 140.
39 G. Landrum, *YAeHMOP- Yet Another Extended Hückel Molecular Orbital Package* (1.1), Cornell University, Ithaca, NY, 1995.
40 M.-H. Whangbo, M. Evain, T. Hughbanks, M. Kertesz, S. Wijeyesekera, C. Zheng and R. Hoffmann, *EHMACC* North Carolina State University, Raleigh, NC, 1987.
41 J. H. Ammeter, H.-B. Bürgi, J. C. Thibeault and R. Hoffmann, *J. Am. Chem. Soc.*, 1978, **100**, 3686.
42 A. Vela and J. L. Gázquez, *J. Phys. Chem.*, 1988, **92**, 5688.
43 S. Alvarez, *Table of parameters for Extended Hückel Calculations*, Universitat de Barcelona, 1995.
44 R. Ramírez and M. C. Böhm, *Int. J. Quantum Chem.*, 1986, **30**, 391.
45 R. Ramírez and M. C. Böhm, *Int. J. Quantum Chem.*, 1988, **34**, 571.
46 H. Wong, J. S. O. Evans, S. Barlow and D. O'Hare, *J. Chem. Soc., Chem. Commun.*, 1993, 1589.

Paper 8/02240B; *Received* 23rd *March*, 1998